Appl. Phys. B 80, 727–731 (2005)
DOI: 10.1007/s00340-005-1788-3

Applied Physics B
Lasers and Optics

L. GUNDLACH[1,✉]
R. ERNSTORFER[1]
E. RIEDLE[2]
R. EICHBERGER
F. WILLIG[1]

Femtosecond two-photon photoemission at 150 kHz utilizing two noncollinear optical parametric amplifiers for measuring ultrafast electron dynamics

[1]Hahn-Meitner-Institute Berlin, SE4 Dynamics of Interfacial Reactions, Glienicker Straße 100, 14109 Berlin, Germany
[2]LS für BioMolekulare Optik, Ludwig-Maximilians-Universität, Oettingenstr. 67, 80538 München, Germany

Received: 22 December 2004 /
Revised version: 15 February 2005 /
Published online: 30 March 2005 •

ABSTRACT An improved setup for femtosecond two-photon photoemission spectroscopy (TR-2PPE) is presented. Two noncollinear optical parametric amplifiers (NOPA) were operated simultaneously at a repetition rate of 150 kHz. The frequencies of the NOPA outputs were tuned such that subsequent second harmonic generation (SHG) provided the two different ultraviolet wavelengths required for the pump and probe pulse. The width of the crosscorrelation function (CC) for pump and probe pulse was sub-30 fs (FWHM).

The performance of this assembly was tested by measuring the lifetime of image potential states (IS) on Cu(111) and Ag(111) surfaces. We present here for the first time lifetimes of the IS that were determined directly from the measured decay of the 2PPE signal.

PACS 42.65.Ky; 79.60.BM; 78.47.+p

1 Introduction

Time-resolved two-photon photoemission (TR-2PPE) is the method of choice for investigating ultrafast photo-driven interfacial processes in the time domain, provided the respective interface can be exposed to ultra-high vacuum [1–5]. The TR-2PPE measurement collects simultaneously information on the energy distribution of the photogenerated electrons and the time evolution of the intermediate state population near the interface. The 2PPE method offers unequaled sensitivity when compared with other pump-probe techniques, e.g., transient absorption, since the photoemitted electrons are counted directly by the detector. Hitherto, two different types of laser sources were employed for 2PPE measurements. On the one hand, high repetition rate laser sources, i.e., systems operating at 100 kHz to MHz repetition rate were used that deliver fairly long pulses with often limited tunability based on optical parametric amplification (OPA) for frequency tuning or harmonic generation. On the other hand, low repetition rate laser sources with repetition rates up to 1 kHz and with a large number of photons per pump pulse were employed. The latter systems render slow signal accumulation; however, the superior noncollinear optical parametric amplification (NOPA) technology [6, 7] can provide extremely short and highly tunable pulses. Recently, tunable sub-20 fs ultraviolet pulses have been achieved with appropriate chirp management in the visible [8]. We report here on a significant improvement of the laser source for 2PPE measurements by adapting the NOPA scheme [9, 10] to operation at 150 kHz repetition rate. Furthermore, a second NOPA was operated simultaneously with one common pump system by utilizing the 400 nm pump pulse for the first NOPA a second time. In this way two independently tunable ultrafast light sources became available.

The improved tunability and shorter duration of the two laser pulses were tested in 2PPE measurements probing the lifetime of image potential states at Cu(111) and Ag(111) surfaces. Image potential states at metal surfaces have been studied extensively ([4, 11] and references herein). Most low-index surfaces of noble-metals exhibit a surface-projected bandgap at $\bar{\Gamma}$. An electron in front of such a surface is trapped by the induced image potential on one side and the bandgap on the other side. The resulting potential generates a Rydberg-like series of bound states in the surface normal direction. These states can be optically populated from the occupied surface state (SS) either resonantly or off-resonantly by quasi-elastic scattering [12]. The main decay channel for the excited image potential state (IS) is governed by the overlap of the IS with the bulk [13]. Previous 2PPE studies revealed a lifetime for the $n = 1$ IS on Cu(111) of 18 ± 5 fs [12]. TR-2PPE studies by Schoenlein et al. indicate lifetimes of less then 20 fs for the $n = 1$ and $n = 2$ image potential state of Ag(111), respectively [14]. More recently, Lingle et al., have reported 32 ± 10 and sub-20 fs for the $n = 1$ and $n = 2$ image potential state of the same system, respectively [15]. The pulse durations in the above experiments were up to six times longer than the reported lifetimes. The values had been extracted from the measurements by fitting the data with optical Bloch equations.

✉ Fax: +49 130 8062-2434, E-mail: gundlach@hmi.de

This method relies on the exact knowledge of time zero, i.e., the time of maximum overlap between pump and probe pulse.

With the improved laser setup described in this paper, it was possible to obtain the IS lifetimes directly from the clear deviations of the measured signals from the crosscorelation (CC) trace and to extract time constants as short as 12 fs by means of optical Bloch equations as well as by fitting with a simple rate model. The time scale of the thus measured lifetimes is in good agreement with values deduced earlier by other groups.

2 Experiment

The femtosecond laser system was based on a commercially available 150 kHz Ti:sapphire amplifier system operating at 800 nm with a pulse energy of 7.5 μJ, which was used to pump two NOPAs. The NOPA principle [9], commonly used for laser systems of low repetition rate and high pulse energy, was recently adapted to a high repetition rate, low pulse energy Ti:sapphire laser [10, 16]. Tunable sub-20 fs pulses in the visible and 15 fs pulses from second harmonic generation (SHG) of the NIR output were obtained.

The Cu(111) and Ag(111) crystals were prepared by cycles of Ar^+ ion bombardment (500 eV, 6 μA, 10 min) and heating at 800 and 700 K, respectively, for 10 min.

The measurement chamber (base pressure 2×10^{-10} mbar) was equipped with a time of flight (TOF) spectrometer with an angular acceptance of ±3.5°. Measurements were carried out in normal emission with an angle of incidence for the light pulses of 45° with respect to the sample surface. All measurements were made at room temperature with both pulses *p*-polarized.

3 Results and discussion

3.1 *NOPA*

The NOPA setup is illustrated in Fig. 1. The first NOPA (upper part of the figure) was pumped with 90% of the Ti:sapphire amplifier output power [10]. The remaining 10% of the fundamental output were used to generate a single filament white light continuum in a 3 mm sapphire plate. The residual 400 nm light not used in the first NOPA process was recollimated with lens L (focal length: 20 cm) and focused with the concave mirror M (radius of curvature: 37.5 cm). The 2 mm BBO crystal was placed in the focal plane of M where pump pulse and white light continuum overlapped with an internal angle of about ±3.7°. As the 400 nm pump pulse was reduced in power and the spatial mode was slightly distorted due to the first conversion process, the second NOPA yielded less pulse energy than the first. Typically NOPA1 generated pulse energies of about 100 nJ in the NIR where usually lower output is observed [9, 10], NOPA2 100 nJ in the visible. The spectral width and the compressibility were quite comparable.

The output of both NOPAs was compressed with standard fused silica prism compressors and frequency doubled to obtain the required ultraviolet wavelengths. Compression was done prior to the SHG processes. This turned out to be more convenient than compression of the SHG output itself [17]. As the pulse had to be down-chirped to precompensate for all dispersive media following the SHG process, the efficiency of the SHG process was reduced. To keep this effect small, as little dispersive elements as possible were inserted in the beam between SHG and sample. Typically 30 nJ were available from the frequency doubled NOPA1 and 4 nJ from doubling of NOPA2.

Figure 2 shows spectra of the NOPA and SHG outputs and autocorrelation (AC) traces of the SHG output as well as the crosscorrelation trace of 280 nm pulses with the 435 nm pulses. As can be seen in Fig. 2, a nearly the full bandwidth of the fundamental NIR pulse generated in NOPA1 is converted to the blue resulting in a 14 fs pulse (see Fig. 2b). The acceptance bandwidth of BBO drops for UV output. As a consequence only a limited part of the visible output of NOPA2 is converted to the UV (Fig. 2c) even though a crystal as thin as 75 μm was used. This limitation has recently been circumvented with much higher effort by achromatic frequency doubling, resulting in sub-10 fs pulses in the UV [18].

AC traces of the 435 nm pulse were taken with a SiC photodiode [19], the autocorrelation of the 325 nm pulse (see Fig. 2d) and the crosscorrelation of the 435 nm pulses with the 280 nm pulses (see Fig. 2e) were measured via the non-resonant TR-2PPE on a Cu (111) single crystal or on a gold sample. The UV pulse length of about 20 fs and

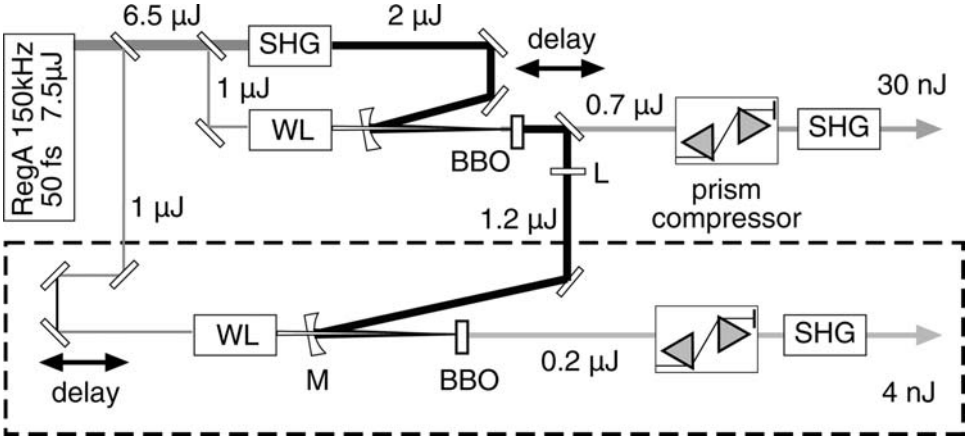

FIGURE 1 Setup for two 150 kHz NOPAs pumped with one 400 nm SHG pulse. The second NOPA is shown inside the dashed box (*dashed box*). See text for details

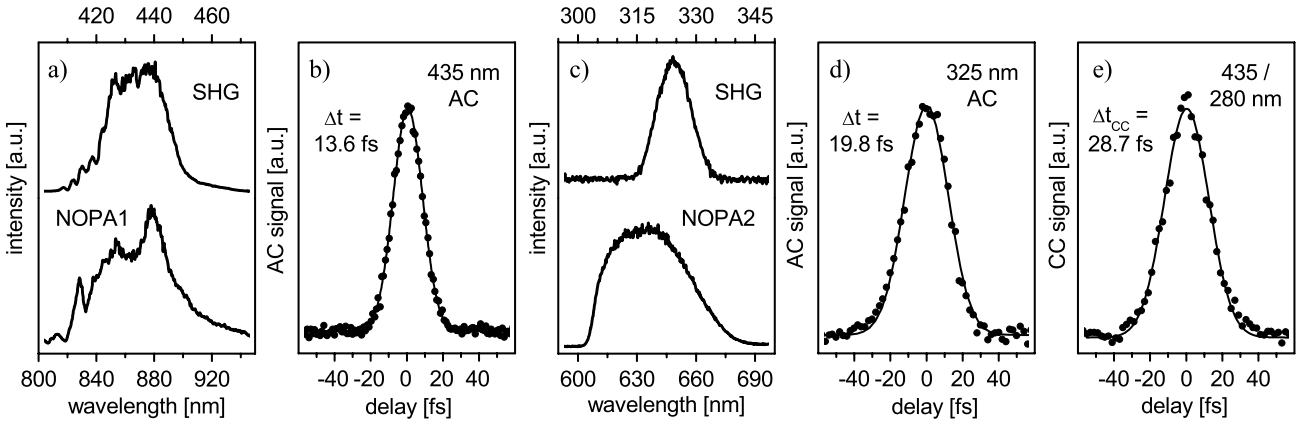

FIGURE 2 Fundamental and SHG spectra for **a** 865/435 nm and **b** 640/325-nm pulses. Autocorrelations are shown for **b** 435 nm and **d** 325 nm. **e** Crosscorrelation of 435 nm and 280-nm pulses (together with fitted Gaussian and FWHM)

the sub-30 fs crosscorrelation between the UV and blue pulses are the shortest values reported for high repetition rate systems so far. Similar ACs were obtained for wavelengths between 270 and 330 nm.

3.2 *Cu(111)*

The relevant energy levels together with the 2PPE process for Cu(111) are depicted in Fig. 3. The $n = 1$ IS can be populated from the occupied $n = 0$ SS either directly when the pump wavelength is in resonance with the transition frequency or indirectly by quasi-elastic scattering of electrons with $K_{||} \neq 0$ when the pump wavelength is off resonance with the SS-IS transition [12]. In the latter case the 2PPE spectrum shows two peaks, one representing resonant excitation of the image potential state, the other nonresonant 2PPE from the occupied surface state. As the intermediate state in the latter process is virtual, TR-2PPE reproduces the crosscorrelation trace of the pulses. Thus it is possible to measure t_0 (coincidence of pump and probe pulse) and the CC trace simultaneously with the temporal evolution of the IS.

For obtaining well separated surface- and image potential state contributions in the spectra, the pump wavelength was tuned to 325 nm (3.8 eV). The probe wavelength was 435 nm (2.8 eV).

The pulse energies were 0.1 and 0.2 nJ for pump and probe pulse, respectively. Figure 4 shows transients for the image potential- and surface state together with fitted curves. The AC trace (20 fs pulse) of the 325 nm pulse was taken from the high energy part of TR-2PPE on a polycrystalline gold sample.

Fits for both transients were performed following Hertel et al. [3]. Briefly, the population of the intermediate state was modeled by means of the optical Bloch equations in the dipole and rotating frame approximation:

$$\frac{\mathrm{d}}{\mathrm{d}t}\rho_{22}(t) = -\frac{1}{T_1}\rho_{22}(t) + \frac{\mu_{12}E_{\mathrm{pump}}(t)}{2i\hbar}\left(\rho_{12}(t) - \rho_{21}(t)\right)$$
$$\frac{\mathrm{d}}{\mathrm{d}t}\rho_{12}(t) = \left(i\delta - \frac{1}{T_2}\right)\rho_{12}(t) + \frac{\mu_{12}E_{\mathrm{pump}}(t)}{2i\hbar}\left(\rho_{22}(t) - \rho_{11}(t)\right) \quad (1)$$

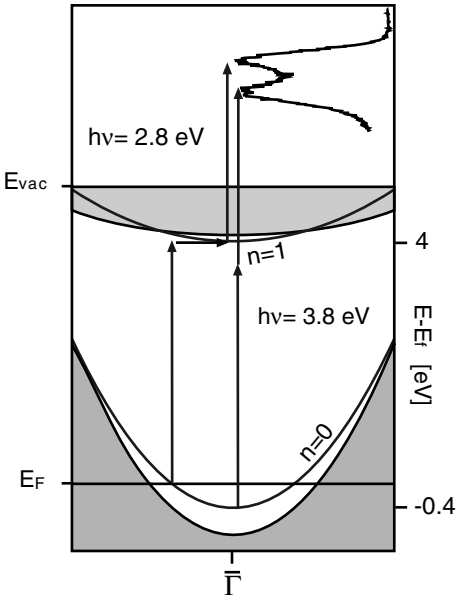

FIGURE 3 Surface projected bulk band structure and dispersion of the $n = 0$ surface state and $n = 1$ image potential state together with the TR-2PPE scheme for the Cu(111) surface. Effective electron masses and binding energies taken from [20]

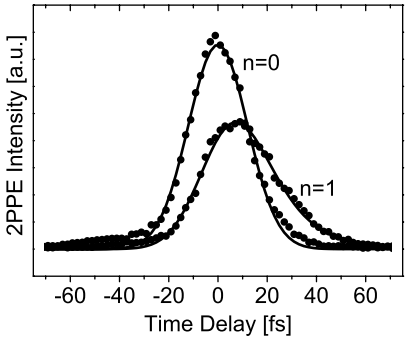

FIGURE 4 Transients for the $n = 0$ surface state and $n = 1$ image potential state at Cu(111) together with the fitted curves obtained from the Bloch model

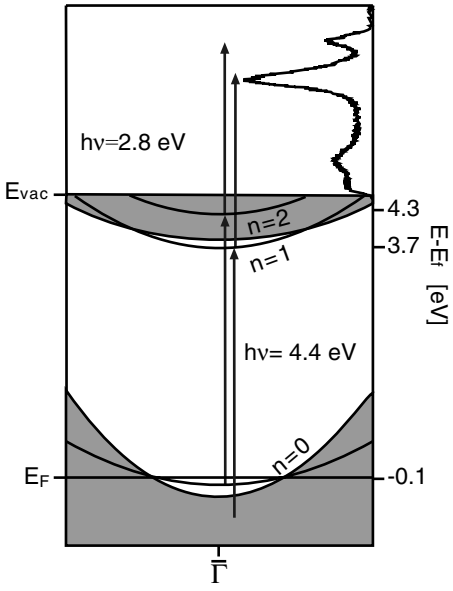

FIGURE 5 Surface projected bulk band structure and dispersion of the $n = 0$-surface state, $n = 1$ and $n = 2$ image potential state together with the TR-2PPE scheme for the Ag(111) surface. Effective electron masses and binding energies taken from [22] and [23], respectively

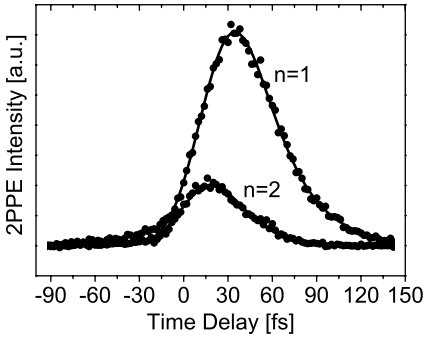

FIGURE 6 Transients for the $n = 1$ and $n = 2$ image potential state at Ag(111) together with the fitted curves obtained from the Bloch model

$1/T_1$ and $1/T_2 = 1/2T_1 + 1/T_2^*$ are the decay and dephasing rates, respectively, and T_2^* is the pure dephasing time. $E_{\text{pump}}(t)$ is the temporal envelope of the pump field and the field strength was kept sufficiently low in accordance with the experiment. The photoemission step was considered by convoluting the intermediate state population with the probe pulse. The SS was fitted with a detuning of $\delta = 400$ meV between resonance and laser frequency to determine t_0 and the width of the pump pulse. With these values at hand, the dephasing and decay rates for the IS were obtained by fitting the transient with the same model assuming resonant excitation (Fig. 4). This gives a lifetime of $T_1 = 12 \pm 2$ fs and a dephasing time of sub-1 fs. The very fast dephasing is attributed to a poor surface order connected with the history of the sample. The sample was routinely used for pulse-correlation measurements and treated with cycles of ion bombardment and heating as a daily routine. In quantum-beat experiments, it has been shown that surface defects strongly influence the dephasing time whereas the life time changes only slightly [21]. Nevertheless, decay rates are affected by the surface quality [11] and the reported lifetimes should be taken with care. Due to the very fast dephasing, the difference between the Bloch model and rate equations is negligible. Thus fitting with a rate model gives the same lifetime.

3.3 *Ag(111)*

The band structures of copper (Fig. 3) and silver (Fig. 5) surfaces are quite similar. But due to the higher lying $n = 0$ surface state and the lower workfunction, it is possible to resonantly populate the $n = 2$ IS [23] and thus strongly enhance its emission.[1] With a pump pulse tuned in resonance with the $n = 0 - n = 2$ transition (280 nm) the TR-2PPE spectra show two peaks. One at higher energies originating from the resonant process and another for the $n = 1$ IS populated non-resonantly from states below the Fermi level. In contrast to the measurement on Cu(111), it is not possible to measure the crosscorrelation trace and t_0 simultaneously with the lifetimes of the image potential state under these conditions. Therefore, the CC trace and t_0 were obtained from the TR-2PPE signal of highly excited electrons in a polycrystalline gold sample prior to the measurement on Ag ($\text{CC}_{280+435} = 33$ fs $\text{FWHM}_{\text{Gauss}}$).

The data analysis was identical to that described for Cu(111). The pulse width and t_0 were determined from measurements on the gold sample. Values of the lifetime and the dephasing time were obtained by fitting the measured curves (Fig. 6) to the solution of Eq. (1). This results in values for the lifetime of 25 ± 2 fs and 18 ± 2 fs for the $n = 1$ and $n = 2$ IS, respectively. These values are in excellent agreement with the values reported earlier by other groups [14, 15]. The dephasing time had to be fixed at $T_2 = 2T_1$ to reproduce t_0, indicating that pure dephasing is much slower than the population decay. However, even a simple rate model reproduces both lifetimes within the error limits as long as t_0 is kept as a free parameter in the model.

4 Summary

A novel setup for two simultaneously driven tunable NOPAs with subsequent SHG at the high repetition rate of 150 kHz was presented, providing sub-20 fs pulses in the UV as well as in the visible.

This setup was tested by time resolving the ultrafast population decay of image potential states on the Cu(111) and Ag(111) surface. The light pulses of the new NOPA setup were sufficiently short for extracting the lifetimes directly from the exponentially decaying slope of the transients. The measured lifetimes of 25 ± 2 fs and 18 ± 2 fs for the $n = 1$ and $n = 2$ image potential state on the Ag(111), respectively, and 12 ± 2 fs for the $n = 1$ image potential state on the Cu(111) surface are in good agreement with previously reported results.

The fully tunable ultraviolet and visible spectrometer with sub-20 fs pump and probe pulses will allow not only 2PPE but many other pump-probe measurements of the very fastest dynamics in physics, chemistry and even light-sensitive biological systems.

[1] The resonance energy for the $n = 2$ IS on Cu(111) is $h\nu = 5.1$ cV.

ACKNOWLEDGEMENTS Financial support by the German Science Foundation (SPP 1093) is gratefully acknowledged.

REFERENCES

1 R. Haight, Surf. Sci. Rep. **21**, 275 (1995)
2 H. Petek, S. Ogawa, Prog. Surf. Sci. **65**, 239 (1997)
3 T. Hertel, E. Knoesel, M. Wolf, G. Ertl, Phys. Rev. Lett. **76**, 536 (1996)
4 P. Echenique, R. Berndt, E. Chulkov, T. Fauster, A. Goldmann, U. Höfer, Surf. Sci. Rep. **52**, 219 (2004)
5 L. Töben, L. Gundlach, T. Hannappel, R. Ernstorfer, R. Eichberger, F. Willig, Appl. Phys. A **78**, 239 (2004)
6 T. Wilhelm, J. Piel, E. Riedle, Opt. Lett. **22**, 1494 (1997)
7 G. Cerullo, M. Nisoli, S. De Silvestri, Appl. Phys. Lett. **71**, 3616 (1997)
8 P. Baum, S. Lochbrunner, E. Riedle, Appl. Phys. B **79**, 1027 (2004)
9 E. Riedle, M. Beutter, S. Lochbrunner, J. Piel, S. Schenkl, S. Spörlein, and W. Zinth, Appl. Phys. B **71**, 457 (2000)
10 J. Piel, E. Riedle, L. Gundlach, R. Ernstorfer, R. Eichberger, Opt. Lett. submitted.
11 M. Weinelt, J. Phys.: Condens. Matter **14**, 1099 (2002)
12 M. Wolf, E. Knoesel, T. Hertel, Phys. Rev. B **54**, R5295 (1996)
13 T. Hertel, E. Knoesel, A. Hotzel, M. Wolf, G. Ertl, J. Vac. Sci. Technol. A **15**, 1503 (1997)
14 R.W. Schönlein, J.G. Fujimoto, G.L. Eesley, T.W. Capehart, Phys. Rev. B **43**, 4688 (1991)
15 J.R.L. Lingle, N.-H. Ge, R.E. Jordan, J.D. McNeill, C.B. Harris, Chem. Phys. **205**, 191 (1996)
16 R. Ernstorfer, L. Gundlach, C. Zimmermann, F. Willig, R. Eichberger, E. Riedle, Ultrafast Optics IV: Selected Contributions to the 4th International Conference on Ultrafast Optics (Springer Series in Optical Sciences, vol. 95, 2004).
17 I.Z. Kozma, P. Baum, S. Lochbrunner, E. Riedle, Opt. Exp. **11**, 3110 (2003)
18 P. Baum, S. Lochbrunner, E. Riedle, Opt. Lett. **29**, 1686 (2004)
19 S. Lochbrunner, P. Huppmann, E. Riedle, Opt. Comm. **184**, 321 (2000)
20 N.V. Smith, Phys. Rev. B **32**, 3549 (1985)
21 M. Weinelt, C. Reuß, M. Kutschera, U. Thomann, I.L. Shumay, T. Fauster, U. Höfer, F. Theilmann, A. Goldmann, Appl. Phys. B **68**, 377 (1999)
22 K. Giesen, F. Hage, F.J. Himpsel, H.J. Riess, W. Steinmann, N.V. Smith, Phys. Rev. B **35**, 975 (1987)
23 K. Giesen, F. Hage, F.J. Himpsel, H.J. Riess, W. Steinmann, Phys. Rev. Lett. **55**, 300 (1985)